CrossMark

Undrained Vertical Bearing Capacity Factors for Ring Shallow Footings

Sadok Benmebarek · Insaf Saifi · Naima Benmebarek

Abstract In this paper, numerical computations using FLAC code are carried out to evaluate the effects of both the ratio of internal radius to external radius 'r_i/r_o' of the ring footing and the embedment ratios up to unity on the undrained bearing capacity factor 'N_c'' for different roughness conditions. It is observed that for both smooth and rough surface ring footings, hardly any reduction occurs in the value of N_c' with an increase in the ratio r_i/r_o up to 0.25. Whereas for $r_i/r_o > 0.25$, the values of N_c' decrease significantly with increasing r_i/r_o. However, for embedded ring footing with rough sides, the results indicate that the bearing capacity difference between circular and ring footings decreases with increase of the embedment depth. For instance, for $r_i/r_o = 0.5$, the difference vanishes completely for embedment ratio >0.5. The results from the analysis compare reasonably well with available theoretical data from the literature.

Keywords Numerical modeling · Ring footing · Bearing capacity · Clay · Failure

1 Introduction

Ring footings are widely used to support structures such as chimneys, silos, television antennas, storage tanks, and bridge piers. The use of ring footings decreases the amount of material used and is more economical. Safe and economical design of such footings requires a good knowledge of both the settlement and bearing capacity relating to ring footings. The bearing capacity of strip and circular footings has been extensively studied for many decades. However, few attempts have been made to study the bearing capacity of ring footings. A very few experiments have also been performed to determine the bearing capacity of ring footings (Saha 1978; Saran et al. 2003). Boushehrian and Hataf (2003) have carried out a finite element analysis to determine the load deformation response of rigid ring footings. Kumar and Ghosh (2005) have investigated the bearing capacity factor N_γ for both smooth and rough ring footings by using the method of characteristics assuming that the interface friction angle between the footing base and the underlying soil mass increases gradually from zero along the footing centerline to along the footing base. By using the finite difference method, Zhao and Wang (2008) have computed N_γ for ring footing in cohesionless soil and found that the value of N_γ decreased significantly with an increase in radius ratio. Choobbasti et al. (2010) have performed a numerical study using Plaxis software to evaluate the

S. Benmebarek (✉) · I. Saifi · N. Benmebarek
NMISSI Laboratory, Civil Engineering and Hydraulic Department, Biskra University, BP 145, 07000 Biskra, Algeria
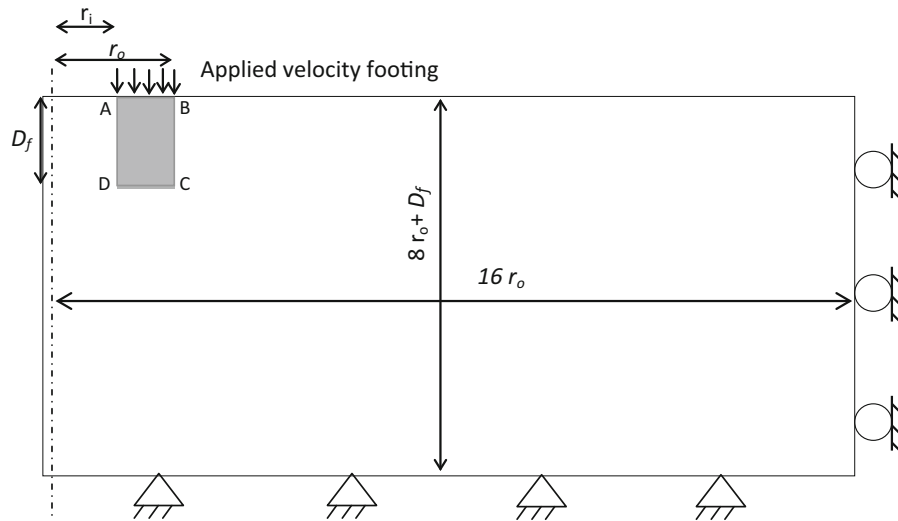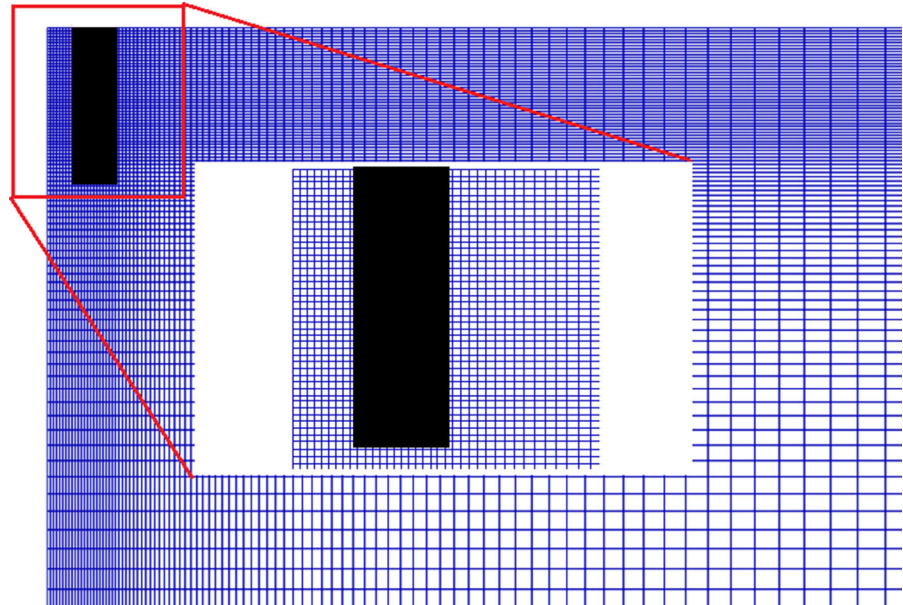e-mail: sadok_benmebarek@yahoo.com

Fig. 1 Model boundary conditions

Fig. 2 Mesh used in FLAC simulations, $D_f/D = 1$

bearing capacity and settlement of a ring footing for a friction soil of $\varphi = 26°$. Numerical computations using FLAC code were carried out by Benmebarek et al. (2012) to evaluate the soil bearing capacity factors N_γ' for both smooth and rough ring footings for low and high friction associated and non-associated Mohr–Coulomb soils. Recently, Kumar and Chakraborty (2015) have examined the bearing capacity factors N_c, N_q and N_γ for smooth and ring footing by employing the lower and upper bound theorems of the

limit analysis in conjunction with finite elements and linear optimization.

Nevertheless, it can be pointed out that previous work relating to ring footings did not deal with the effect of embedment on the undrained bearing capacity which seems to be more suitable and economical for axi-symmetric structures such as silos, chimneys, and storage tanks. In this context, the aim of this work is to carry out numerical computations using the software Fast Lagrangian Analysis of Continua

(FLAC) (2007) to evaluate the effects of both the internal radius to external radius (r_i/r_o) of the ring footing and the embedment ratios up to unity on the undrained bearing capacity factor N'_c for different base and side roughness conditions in homogeneous undrained soil. The computational results are compared with previous published results available in the literature.

2 Numerical Modelling Procedure

This paper deals with the numerical study of bearing capacity of ring embedded footing with internal and external radius r_i and r_o respectively, and subjected to an axial static load. Owing to the difficulty of the prediction of the bearing capacity load due to the sensitivity to the grid refinement around the ring footing base when r_i/r_o converge to unity, the present results are limited to $r_i/r_o = 0.90$. The computations have been done for the values of the r_i/r_o ratio 0, 0.25, 0.33, 0.50, 0.625, 0.75 and 0.90. These cover most problems of practical interest.

On account of the symmetry about a vertical line passing through the center of the footing, an axisymmetric analysis was performed with FLAC code. The bottom boundary was assumed to be fixed, and the vertical boundaries were constrained in motion in the horizontal direction. In order to develop an acceptable analysis scheme for later computations, preliminary simulations have been carried out, by testing the size of the domain and the grid refinement. The geometry and boundary conditions retained for these computations are shown in Fig. 1. The vertical and bottom boundaries located at a distance of $D_f + 8r_o$ and $16r_o$ respectively were found sufficient to avoid boundary effects on the computation of the undrained bearing capacity factor N'_c. Footing embedment depth to footing diameter ratio D_f/D was varied from 0 (footing at the ground surface) to 1. Both soil and rigid footing were discretised. Interface elements defined by Coulomb shear-strength criterion encoded in FLAC were placed between soil and footing along the boundary 'ABCD' (Fig. 1) to simulate different interface conditions, rough and smooth interfaces base 'CD' and vertical sides of the footing 'BC' and 'AD' were considered. The case of a smooth base and smooth sides was considered to provide a lower limit

to the bearing capacity factor. A rough sides and base may be an appropriate assumption for a solid concrete foundation. This interface conditions were assumed in order to verify and evaluate the results of the present study with previous published results available in the literature using different methods.

The model domain for this study is shown in Fig. 2. In the vicinity of the footing, the grid is refined to capture the large gradients in strain. The highest strain gradient will be in the region adjacent to the left and right sides of the part of the footing located between the internal radius and the external radius. The grid is therefore very fine in this area.

In order to be consistent with existing design expressions and the comparative studies described above, the soil mass assumed weightless (essentially taking the foundation and soil unit weights as identical) was modeled using the Mohr–Coulomb constitutive model. A constant undrained strength, $C_u = 100$ kPa with $\varphi_u = 0°$, a Young's modulus, E, of 50 MPa and a Poisson's ratio, v, of 0.499 were assigned to the soil. It is noteworthy that the undrained bearing capacity of foundations is insensitive to the stiffness of soils (Yun and Bransby 2007; Shaiu et al. 2011) and the soil unit weight as described by Houlsby and Martin (2003) and verified in preliminary simulations.

Interfaces were defined with null friction, cohesion, normal and shear stiffness of 1e9 kN/m^3. To model the rough soil/footing interface, the same soil undrained strength was assigned to interface elements. In the case of a smooth interface, the interface elements were assigned null undrained strength (0 kPa), such that

Table 1 Bearing capacity factor N'_c for embedded circular footings ($r_i/r_o = 0$)

D_f/D	Present solution FLAC ($r_i/r_o = 0$)			
	SS–SB	RS–RB	RS–SB	SS–RB
0	5.66	6.04	5.66	6.04
0.1	6.68	7.12	7.08	6.81
0.2	7.17	8.05	8.03	7.21
0.3	7.53	8.80	8.85	7.55
0.5	8.10	10.31	10.30	8.11
1	9.25	13.41	13.40	9.25

SS smooth-side, *SB* smooth-base, *RS* rough-side, *RB* rough-base, *LB* lower bound, *UB* upper bound
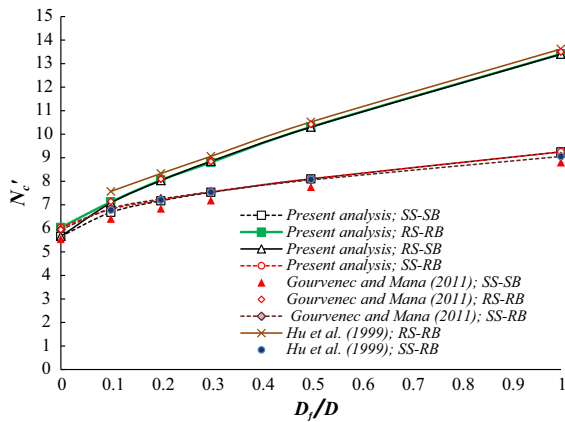
Fig. 3 A comparison of the variation of N_c' with D_f/D for a circular footing

there was essentially no shear stress mobilized along the side of the footing.

The loading of footings was simulated by imposing equal vertical velocities to the nodes of the footing surface represented by the boundary '*AB*' (Fig. 1) until reaching failure. After running a number of verifications, the magnitude of vertical velocities is finally chosen to be 1×10^{-7} m/s downward, which is small enough to minimize the influence of initial velocity to the results (FLAC).

Using a FISH function, the ultimate bearing capacity q_u was calculated by dividing the computed ultimate total vertical load by the area of the footing. It was pointed out that the load was calculated as the sum of the vertical reaction forces along the footing level '*AB*' as expressed by Eq. (1). This load includes the resistance from both the base and the vertical sides of the footing.

Table 2 Bearing capacity factor N_c' for smooth and rough ring footings, $D_f/D = 0$

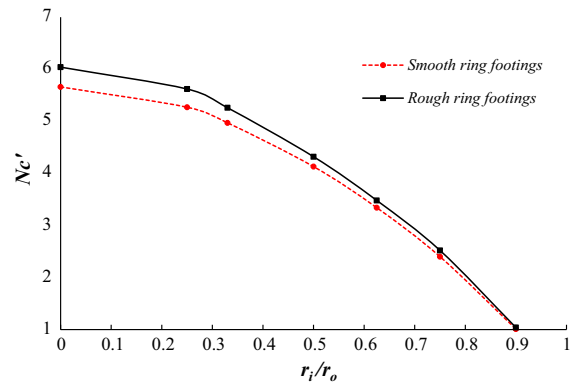| r_i/r_o	Smooth ring footings	Rough ring footings
0	5.66	6.04
0.25	5.27	5.62
0.33	4.97	5.26
0.50	4.13	4.32
0.625	3.34	3.48
0.75	2.40	2.52
0.9	1.01	1.04

Fig. 4 Variation of the bearing capacity factor N_c' with r_i/r_o for both smooth and rough footing, $D_f/D = 0$

$$q_u = \frac{2\pi \sum f_k r_k}{\pi r_0^2} = \frac{2 \sum f_k r_k}{r_0^2} \tag{1}$$

where q_u ultimate bearing capacity; f_k the reaction force in the vertical direction at footing grid point k; r_k associated radius at grid point k; r_0 radius of the footing.

For undrained clays, the ultimate bearing capacity equation has the following form:

$$q_u = s_c d_c N_c C_u = N_c' C_u \tag{2}$$

where s_c is the shape factor, d_c is the depth factor, C_u is the undrained shear strength, N_c is the bearing capacity factor corresponding to strip footing, and N_c' is the bearing capacity factor corresponding to circular or ring footings with D_f depth.

Hence, from Eq. (2), the bearing capacity factor can be deduced from the following expressions:

$$N_c' = \frac{q_u}{C_u} \tag{3}$$

3 Results and Discussion

Compared with strip and circular footings, only limited studies are available that deal exclusively with ring footings. Nevertheless, it can be pointed out that most works have focused on surface ring footings resting on cohesionless frictional soil. However, the undrained bearing capacity of ring footings embedded in cohesive soil has not been discussed in the open literature and no exact solution has been identified. Accordingly, the ultimate bearing capacity of

Table 3 Bearing capacity factor N'_c for ring footing

D_f/D	Present solution FLAC											
	$r_i/r_o = 0$				$r_i/r_o = 0.5$				$r_i/r_o = 0.75$			
	SS–SB	RS–RB	RS–SB	SS–RB	SS–SB	RS–RB	RS–SB	SS–RB	SS–SB	RS–RB	RS–SB	SS–RB
0	5.66	6.04	5.66	6.04	4.13	4.30	4.13	4.32	2.40	2.52	2.40	2.52
0.1	6.68	7.12	7.08	6.81	5.35	5.94	5.95	5.45	3.55	4.11	4.10	3.64
0.2	7.17	8.05	8.03	7.21	5.55	7.13	7.13	5.69	3.58	5.13	5.10	3.73
0.3	7.53	8.80	8.85	7.55	5.57	8.18	8.18	5.84	3.59	6.10	6.08	3.74
0.5	8.10	10.31	10.30	8.11	5.61	10.05	10.02	6.00	3.59	7.99	7.96	3.75
1	9.25	13.41	13.40	9.25	5.61	13.57	13.57	6.05	3.59	12.34	12.33	3.75

D_f/D	Present solution FLAC			
	$r_i/r_o = 0.9$			
	SS–SB	RS–RB	RS–SB	SS–RB
0	1.01	1.04	1.01	1.04
0.1	2.22	2.77	2.76	2.28
0.2	2.28	3.83	3.83	2.33
0.3	2.29	4.81	4.81	2.34
0.5	2.29	6.69	6.69	2.34
1	2.29	11.12	11.12	2.34

embedded up to 1 for circular footing was examined in order to establish the accuracy of the present finite difference analyses and validate the modeling procedure. Numerical results were compared with known solutions (Cox et al. 1961; Eason and Shield 1960; Hu et al. 1999; Gourvenec and Mana 2011).

Firstly, bearing capacity factors for circular surface footing were computed. An N'_c factor of 5.66 was obtained for the smooth circular surface footing, which is 0.5 % in error compared with the well-known (Cox et al. 1961) solution of 5.69. In a similar way, the obtained N'_c factor of 6.04 for a rough circular surface footing is 0.17 % in error compared with the 6.05 solution of Eason and Shield (1960). The accuracy of the present numerical analysis is therefore excellent, being within 1 % of the closed form solutions.

Secondly, bearing capacity factors for circular embedded footing were also computed for $D_f/D = 0, 0.1, 0.2, 0.3, 0.5$ and 1. The results are listed in Table 1 which shows the variation of N'_c with depth embedment and footing-soil interface roughness conditions (SS: perfectly smooth-side, SB: perfectly smooth-base, RS: perfectly rough-side, RB: perfectly rough-base). The results show that the N'_c value is

found to increase for rough side more than smooth side and the effect of footing base roughness decreases with the increase of D_f/D and practically is attenuated at $D_f/D = 1$.

Owing to no availability of results for a ring footing, the computed N'_c values of a circular footing with various combinations of D_f/D are compared with prediction solutions reported in the literature. The obtained values of N'_c were compared with the values computed using the finite element method by Hu et al. (1999) and using finite element and limit analysis by Gourvenec and Mana (2011).

The comparison of all these results is shown in Fig. 3. It can be noted that the present N'_c values are in an excellent agreement with the solutions reported by Hu et al. (1999) and Gourvenec and Mana (2011) and the difference is found to be very marginal, thus besides confirming the accuracy of this finite difference analysis.

Then, the effect of the internal radius to external radius of the ring footing (r_i/r_o) on bearing capacity factor N'_c has been investigated for various combinations of embedment ratio (D_f/D) up to unity and footing-soil interface roughness conditions. The
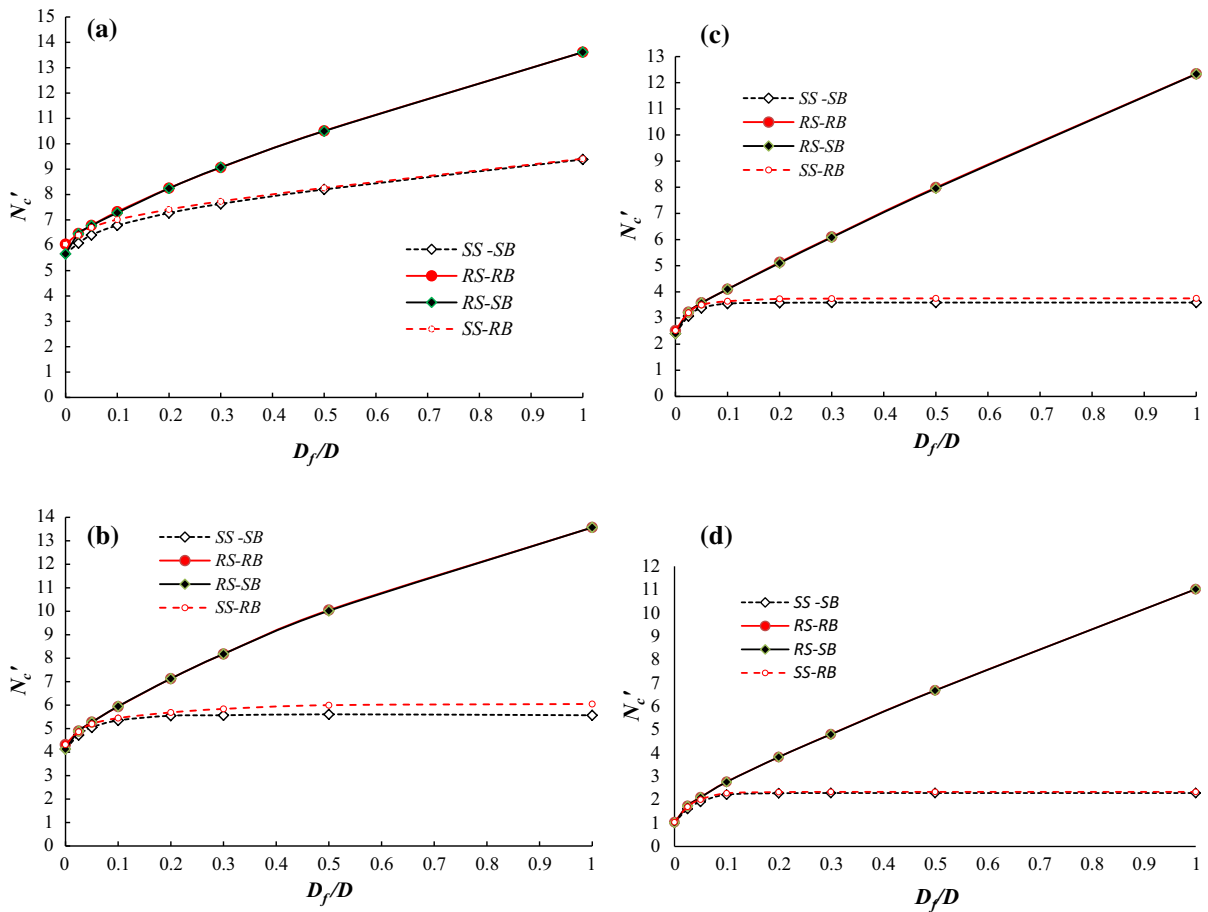
Fig. 5 Variation of N_c' with D_f/D. **a** $r_i/r_o = 0$, **b** $r_i/r_o = 0.5$, **c** $r_i/r_o = 0.75$, **d** $r_i/r_o = 0.9$

computation results of N_c' for surface circular and ring footings with $r_i/r_o = 0, 0.25, 0.33, 0.50, 0.65, 0.75$ and 0.90 are reported in Table 2. Figure 4 illustrates the variation of N_c' with r_i/r_o for smooth and rough surface ring footings. It can be observed that for both smooth and rough surface ring footings, hardly any reduction occurs in the value of N_c' with an increase in the ratio r_i/r_o up to 0.25. Whereas for $r_i/r_o > 0.25$, the decrease of N_c' is more pronounced. From Fig. 4, it can be seen that the N_c' value for rough base is slightly greater than the value for smooth footing base and the difference decreases with the increasing r_i/r_o.

Table 3 provides the obtained values of N_c' of ring footings for various footing-soil interface roughness conditions and embedment depth ratios $D_f/D = 0$, 0.1, 0.2, 0.3, 0.5 and 1. By comparing the roughness effect of the footing base and sides (SS–SB, SS–RB, RS–RB and RS–SB), it can be seen that base

roughness has lightly effect on the magnitude of N_c'. In occurrence the difference is <7 % corresponding to surface footing and decreases with increasing footing depth. However, the side roughness has significant effect on the magnitude of N_c' which increases continuously with the increasing D_f/D. The intermediate side roughness effect was investigated by linking the interface strength properties to the strength properties of the undrained soil. As often used in practice, three strength reduction factor of the interface 1/3, 1/2 and 2/3 were tested. The computation results showed that linear interpolation between perfectly smooth and perfectly rough sides gives a good approximation of the intermediate side roughness effect.

Figure 5 shows the variation of the computed N_c' as a function of embedment ratio D_f/D for different ratios $r_i/r_o = 0$, 0.50, 0.75 and 0.90 which include the contribution of both the footing base and the footing
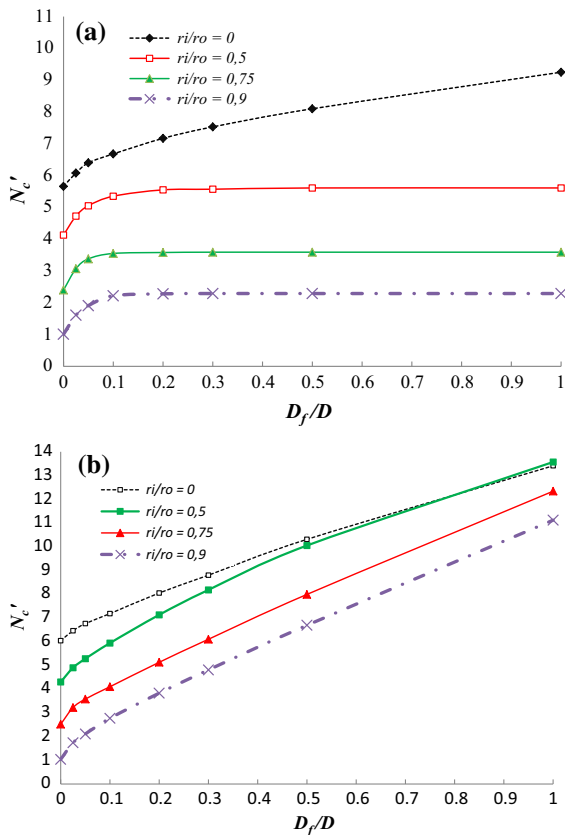
Fig. 6 Variation of the bearing capacity factor N_c' with D_f/D and r_i/r_o for a ring footing. **a** SS–SB, **b** RS–RB

sides for different roughness condition of the footing-soil interfaces. For cases of both ring and circular footing, it can be noted that the results of this study in the case of RS–RB are similar to those obtained in the case of RS–SB. Also, the results in the case of SS-SB are similar to those obtained in the case of SS–RB but for circular footing, the difference is found to be very marginal. Also from Fig. 5, it can be seen that for the case of circular footings with smooth sides (SS–SB and SS–RB) the magnitude of N_c' increases invariably with an increase in D_f/D. However for ring footings $r_i/r_o = 0.50$, 0.75 and 0.90, the magnitude of N_c' increases invariably with an increase in D_f/D up to $D_f/D \approx 0.1$, thereafter, the value of N_c' becomes almost constant. However, for the case of circular and ring footings with rough sides (RS–SB and RS–RB), the magnitude of N_c' increases continuously with an increase in D_f/D. This is attributed to the contribution of sides shear strength to the bearing capacity. The effect of side's roughness on N_c' of ring footing is

illustrated in Fig. 6. Parts (a) and (b) in this figure correspond to SS–SB and RS–RB, respectively. For SS, N_c' value increases to reach a constant value which decrease with increasing r_i/r_o. For RS, the obtained results indicate that the bearing capacity difference between circular and ring footings (Fig. 6a) decreases with increasing D_f/D. For instance, for $r_i/r_o = 0.75$, the difference compared to circular for $D_f/D = 1$ is <20 %. While for $r_i/r_o = 0.50$, the difference vanishes completely for $D_f/D > 0.5$. This observation involves that rather than employing a solid circular footing with rough side, one can even adopt a ring footing by keeping an internal diameter approximately equal to 0.5 times the outer diameter without causing any significant reduction in the magnitude of the collapse load for $D_f/D > 0.5$. From these results, it is interesting to compare the two practical situations of the internal space of the ring footing hollow or filled with soil. Numerical analyses were performed for cases of footing-soil interface roughness condition RS-RB and embedment depth ratio $D_f/D = 1$. For $r_i/r_o = 0.50$, 0.75 and 0.90, the effect of voiding the internal space of the ring footing produces a reduction of 31, 39 and 45 % of the bearing capacity respectively. Therefore, to obtain high bearing capacity of embedded ring footing, it is recommended to fill the interior of the ring footing.

Figures 7 and 8 show a comparison of the displacement vector field according to ultimate state of shear failure between circular ($r_i/r_o = 0$) and ring footing ($r_i/r_o = 0.50$) for cases SB-SS and RS-RB respectively. One can note that as the embedment depth of footings increases, the intensity of the displacements increases and the extent of the displacement field become larger at the inner edges of the ring footing and at the outside limit of circular footing for SS. However, for RS, it can be seen that the displacements are obviously only at the outer edge of the ring footing for $D_f/D \geq 0.5$. As can be seen from Fig. 8 the failure mechanism of ring footing is very similar to that for circular footings when $D_f/D \geq 0.5$.

4 Conclusions

The finite difference FLAC code was used to evaluate the undrained bearing capacity factors N_c' for different roughness condition of the footing-soil interfaces of

Fig. 7 Displacement field
vectors for SS–SB. **a** Ring
footing ($r_i/r_o = 0.5$),
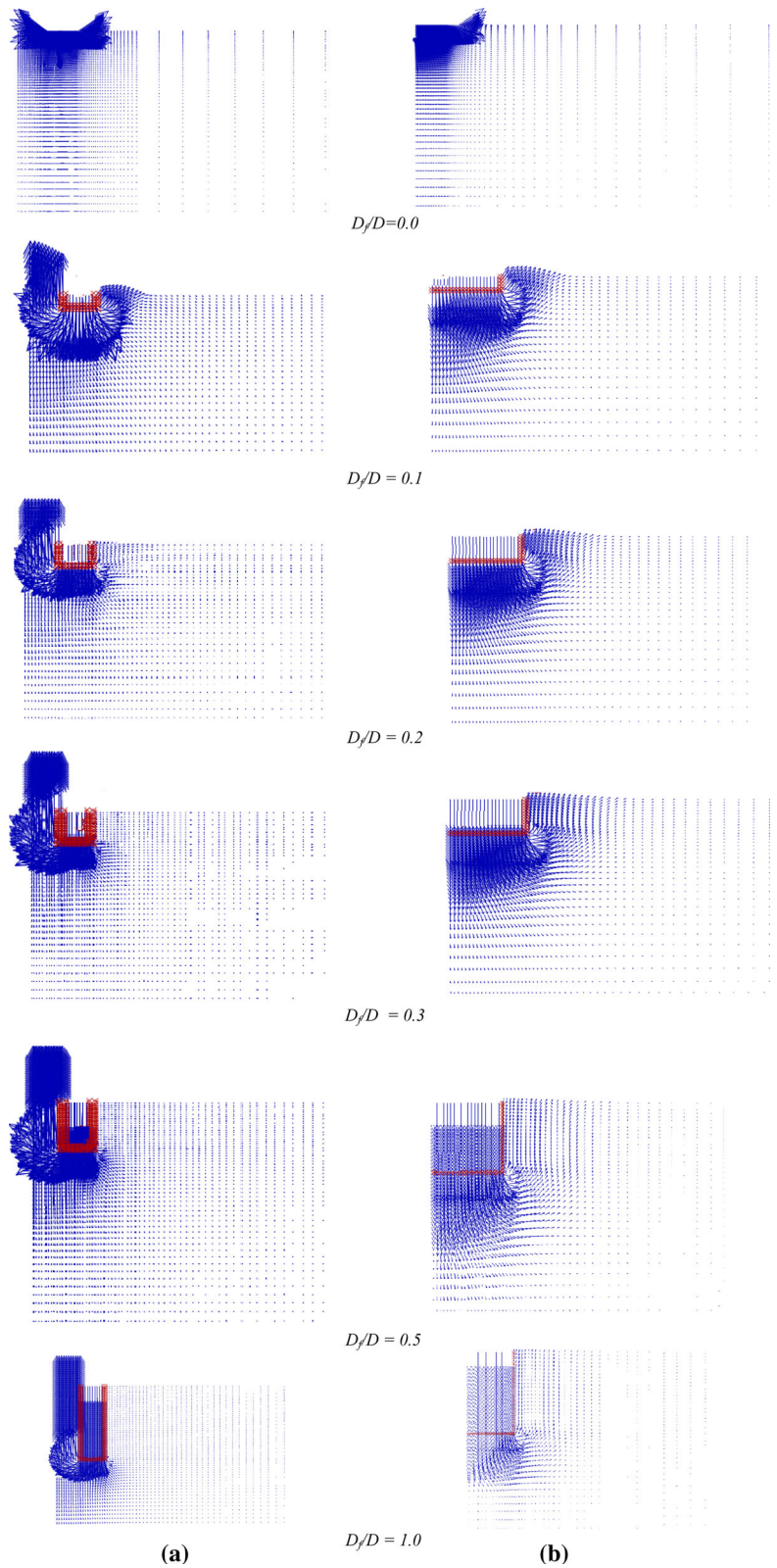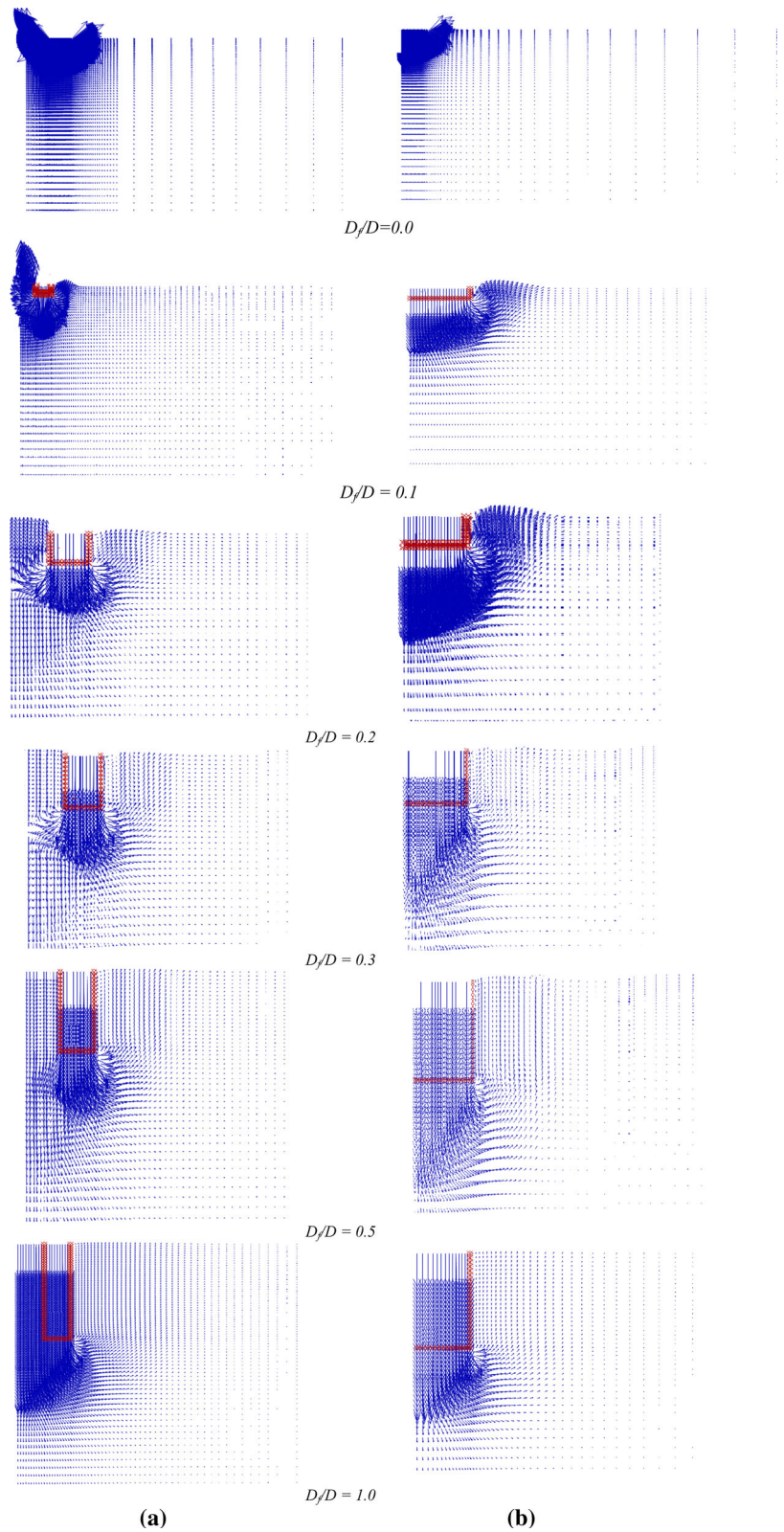**b** circular footing ($r_i/r_o = 0$)

$D_f/D=0.0$

$D_f/D = 0.1$

$D_f/D = 0.2$

$D_f/D = 0.3$

$D_f/D = 0.5$

$D_f/D = 1.0$

(a)

(b)

Fig. 8 Displacement field
vectors for RS–RB. **a** Ring
footing ($r_i/r_o = 0.5$),
b circular footing ($r_i/r_o = 0$)

$D_f/D=0.0$

$D_f/D = 0.1$

$D_f/D = 0.2$

$D_f/D = 0.3$

$D_f/D = 0.5$

$D_f/D = 1.0$

(a)   **(b)**

ring shallow footings. From the comparison with the various studies available in the literature, the following can be concluded:

- The magnitude of N_c' of surface ring footings is found to decrease continuously with an increase in r_i/r_o. In addition, the decrease is more pronounced for r_i/r_o beyond 0.25 for both smooth and rough footings;
- The results indicate that the magnitude of N_c' depends on the roughness of the vertical side of the footing more than the base footing-soil interface roughness. Base footing roughness has low effect on the magnitude of N_c' which decreases continuously with depth. However, the magnitude of N_c' is found to increase continuously with an increase in embedment ratio D_f/D for RS more than circular footing. Thus, embedded ring footing with RS may be economic than circular footing, in occurrence, the results indicate that the N_c' for RS ring footing with $D_f/D > 0.5$ is the same N_c' for circular footing;
- The smooth footing sided limits the increase of N_c' with depth.

References

Benmebarek S, Remadna M, Benmebarek N, Belounar L (2012) Numerical evaluation of the bearing capacity factor of ring footings. Comput Geotech 44:132–138

Boushehrian JH, Hataf N (2003) Experimental and numerical investigation of the bearing capacity of model circular and ring footings on reinforced sand. Geotext Geomembr 21:241–256

Choobbasti AJ, Hesami S, Najafi A, Pirzadeh S, Farrokhzad F, Zahmatkesh A (2010) Numerical evaluation of bearing capacity and settlement of ring footing, case study of Kazeroon cooling towers. Int J Res Rev Appl Sci 4(3):263–271

Cox AD, Eason G, Hopkins HG (1961) Axially symmetric plastic deformations in soils. Philos Trans R Soc Lond Ser A1036:1–45

Eason G, Shield RT (1960) The plastic indentation of a semi-infinite solid by a perfectly rough circular punch. Z Angrew Math Phys 11:33–43

FLAC (2007) Fast lagrangian analysis of continua. Itasca Consulting Group Inc, Minneapolis

Gourvenec SM, Mana DSK (2011) Undrained vertical bearing capacity factors for shallow foundations. Géotech Lett 1:101–108

Houlsby GT, Martin CM (2003) Undrained bearing capacity factors for conical footings on clay. Geotechnique 53(5):513–520

Hu Y, Randolph MF, Watson PG (1999) Bearing response of skirted foundations on non-homogeneous soil. J Geotech Geoenviron Eng 125(12):924–935

Kumar J, Chakraborty M (2015) Bearing capacity factors for ring foundations. J Geotech Geoenviron Eng 141(10):06015007

Kumar J, Ghosh P (2005) Bearing capacity factor Nγ for ring footings using the method of characteristics. Can Geotech J 42:1474–1484

Saha MC (1978) Ultimate bearing capacity of ring footings on sand. M.Eng. thesis. UP, University of Roorkee, India

Saran S, Bhandari NM, Al-Smadi MMA (2003) Analysis of eccentrically–obliquely loaded ring footings on sand. Ind Geotech J 33(4):422–446

Shaiu JS, Merifield RS, Lyamin AV, Sloan SW (2011) Undrained stability of footings on slopes. J Geotech Geoenviron Eng 11:3891–3900

Yun G, Bransby MF (2007) The horizontal-moment capacity of embedded foundations in undrained soil. Can Geotech J 44:409–424

Zhao L, Wang JH (2008) Vertical bearing capacity for ring footings. Comput Geotech 35(2):292–304